Vibrational Spectroscopic and Conformational Analysis of Pinosylvin

Ferenc Billes*

Department of Physical Chemistry, Budapest University of Technology and Economics, H-1521 Budapest, Budafoki út 8., Hungary

Ildikó Mohammed-Ziegler

Institute of Chemistry, Chemical Research Center, Hungarian Academy of Sciences, H-1025 Budapest, Pusztaszeri út 59-67, Hungary

Hans Mikosch

Institute for Solid State Chemistry and Electrochemistry, Vienna University of Technology, A-1060 Vienna, Getreidemarkt 9, Austria

Allan Holmgren

Division of Inorganic Chemistry, Luleå University of Technology, S-97187 Luleå, Sweden

Received: August 18, 2001; In Final Form: April 8, 2002

Infrared and Raman spectra of pinosylvin were recorded and the vibrational frequencies with the corresponding infrared intensities were compared with the results of ab initio calculations utilizing the DFT method with the Becke3P86 functional and the 6-31G(d) basis set. Normal coordinate analysis was carried out. The effect of the conformation of the OH groups on the distribution of net charges, molecular energy and vibrational fundamentals were analyzed. One of the OH-cis−OH-trans conformers has the lowest energy. The conformation has a strong effect on the aforementioned properties, e.g., the cis-to-trans transition generates electron repulsion toward the vinylidene group between the two benzene rings. The changes in the different properties are in good accordance with each other. For comparison, the vibrational spectra were also recorded and calculated for the parent compound, trans-stilbene.

1. Introduction

Pinosylvin (PS, Figure 1) and its 3-O-methyl ester[1,2] play an important role in the self-protection of some trees against fungal decease. Several kinds of trees are able to produce this very useful compound, e.g., in the heartwood of *Pinus*, *Eucaliptus*, and *Maclura* species. PS (3,5-dihydroxy-trans-stilbene) is a derivative of trans-stilbene (TS, Figure 2). The biosynthesis of trans-stilbene derivatives was reported from coumarine-CoA derivatives (resveratrol synthase).[4]

The vibrational spectra of the parent compound (TS) were discussed in detail by several authors during recent years.[5−9] Whereas the biological properties of PS were thoroughly treated, less attention was paid to its structure and spectroscopic properties. The FT-Raman spectrum was found to be applicable for the quantitative determination of PS in wood.[2,3] The mechanism of PS adsorption on different wood species was investigated and presented by Mohammed-Ziegler in her thesis.[10] Additionally, the quality of the adsorption of PS was studied with DRIFT and Raman spectroscopies. To the best of our knowledge, no work dealing with the assignment of the vibrational spectra of PS has been reported so far.

2. Experimental Section

Compound. Pinosylvin was the product of the Phero Tech. Inc., B. C., Canada (>99%) and was applied without any further purification.

* Corresponding author. E-mail: fbilles@mail.bme.hu

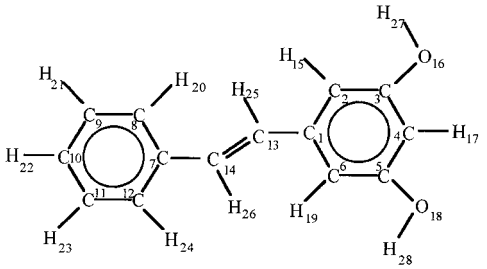

Figure 1. Structure of pinosylvin (HO-trans−HO-trans conformer); the numbers refer to the numbering used in the text.

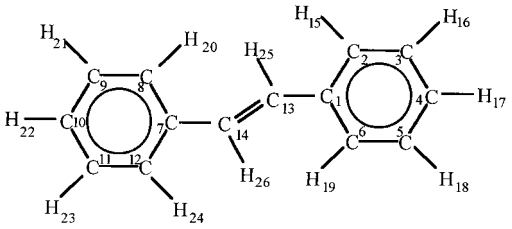

Figure 2. Structure of trans-stilbene; the numbers refer to the numbering used in the text.

Measurements. Infrared spectra (DRIFT) were measured on a Perkin-Elmer System 2000 FT-IR spectrometer with 1 cm^{-1} resolution accumulating 512 scans. The DFT method was chosen because of the expected application of these data. Pinosylvin as a fungicidal compound is a promising preservative on wood.

10.1021/jp013218w CCC: $22.00
Published on Web 06/06/2002

TABLE 1: Measured and Calculated Geometric Parameters of trans-Stilbene (TS) and the Pinosylvin (PS) Conformers[a]

geometric parameter[b]	measured X-ray[c]	calculated [6-31G(d) basis set]							geometric parameter[b]	measured X-ray[c]	calculated [6-31G(d) basis set]						
		RHF[d]	BLYP[e]	B3P86[f]							RHF[d]	BLYP[e]	B3P86[f]				
		TS			CC PS	CT PS	TC PS	TT PS			TS			CC PS	CT PS	TC PS	TT PS
r(C1,C2)	1.403	1.394	1.420	1.404	1.401	1.398	1.404	1.401	φ(C2,C3,C4)	120.0	–	120.1	120.1	120.	120.7	120.5	120.7
r(C1,C6)	1.406	1.394	1.421	1.405	1.40	1.405	1.399	1.402	φ(C2,C3,H/O16)	–	–	–	119.7	117.3	117.	122.5	122.
r(C1,C13)	1.471	1.478	1.470	1.460	1.46	1.461	1.462	1.461	φ(C3,C2,H15)	–	–	–	119.7	118.8	118.	120.0	120.0
r(C2,C3)	1.392	1.384	1.402	1.390	1.392	1.395	1.392	1.39	φ(C3,C4,C5)	119.3	-	119.4	119.	119.1	119.0	119.0	118.8
r(C2,H15)	1.080	1.075	–	1.088	1.085	1.08	1.088	1.088	φ(C3,C4,H17)	–	–	–	120.4	120.5	121.9	119.3	120.6
r(C3,C4)	1.394	1.38	1.405	1.392	1.394	1.391	1.393	1.391	φ(C3,H/O16,H27)	–	–	–	–	109.0	108.8	108.7	108.
r(C3,H/O16)	–	–	–	1.08	1.361	1.360	1.361	1.360	φ(C4,C3,H/O16)	–	–	–	120.2	122.2	122.	116.9	117.
r(C4,C5)	1.396	1.386	1.409	1.395	1.398	1.397	1.395	1.394	φ(C4,C5,C6)	120.7	-	120.6	120.5	120.9	121.	121.1	121.1
r(C4,H17)	–	–	–	1.086	1.090	1.087	1.087	1.08	φ(C4,C5,H/O18)	–	–	–	120.0	121.8	116.5	121.8	116.7
r(C5,C6)	1.392	1.384	1.401	1.388	1.389	1.389	1.392	1.393	φ(C5,C4,H17)	–	–	–	120.2	120.4	119.2	121.8	120.5
r(C5,H/O18)	–	–	–	1.08	1.361	1.361	1.360	1.360	φ(C5,C6,H19)	–	–	–	119.1	118.2	119.5	118.3	119.6
r(C6,H19)	1.080	1.075	–	1.08	1.084	1.087	1.084	1.087	φ(C5,H/O18,H28)	–	–	–	–	109.1	108.6	108.9	108.7
r(C7,C8)	1.403	1.394	1.42	1.405	1.405	1.405	1.405	1.405	τ(C4,C3,C16,H27)	–	–	–	–	0.1	0.1	179.2	179.9
r(C7,C12)	1.406	1.394	1.420	1.404	1.404	1.404	1.404	1.404	τ(C4,C5,C18,H28)	–	–	–	–	0.3	180.0	0.2	180.0
r(C7,C14)	1.471	1.47	1.470	1.460	1.460	1.460	1.460	1.460	τ(C13,C14,C7,C8)*	6.6	23.3	–	0.0	6.4	7.1	7.3	8.0
r(C8,C9)	1.392	1.38	1.401	1.388	1.38	1.388	1.388	1.388	τ(C13,C14,C7,C12)	173.3	157.2	180.0	180.0	173.8	173.1	173.0	172.3
r(C8,H20)	1.080	1.075	–	1.086	1.086	1.08	1.086	1.086	τ(C14,C13,C1,C2)	173.3	157.2	180.0	180.0	173.0	171.3	171.3	169.5
r(C9,C10)	1.394	1.38	1.409	1.395	1.395	1.395	1.395	1.395	τ(C14,C13,C1,C6)**	6.6	23.3	–	0.0	7.1	8.8	8.8	10.6
r(C9,H21)	1.080	–	–	1.087	1.087	1.087	1.087	1.087	τ(H25,C13,C1,C2)	–	–	–	0.0	6.0	7.5	7.5	9.1
r(C10,C11)	1.396	1.386	1.405	1.392	1.392	1.392	1.392	1.392	τ(H25,C13,C1,C6)	–	–	–	180.0	173.9	172.	172.3	170.7
r(C10,H22)	1.080	–	–	1.086	1.086	1.086	1.086	1.086	τ(H25,C13,C14,H26)	–	–	–	180.0	177.8	177.3	177.	176.9
r(C11,C12)	1.292	1.384	1.402	1.390	1.390	1.390	1.390	1.390	τ(H26,C14,C7,C8)	–	–	–	180.0	174.5	174.0	173.8	173.
r(C11,H23)	1.080	–	–	1.087	1.087	1.087	1.087	1.087	τ(H26,C14,C7,C12)	–	–	–	0.0	5.	5.7	6.0	6.4
r(C12,H24)	1.080	1.075	–	1.088	1.088	1.088	1.088	1.088	$\tau^*+\tau^{**}$	13.2	46.6	-	0.0	13.5	15.9	16.1	18.6
r(C13,C14)	1.341	1.328	1.362	1.34	1.346	1.346	1.346	1.346	τ(C4,C3,C16,H27)	–	–	–	–	0.1	0.1	179.2	179.9
r(C13,H25)	1.080	1.077	–	1.089	1.08	1.089	1.089	1.089	τ(C4,C5,C18,H28)	–	–	–	–	0.3	180.0	0.2	180.0
r(C14,H26)	1.080	1.077	–	1.089	1.08	1.090	1.089	1.089	τ(C13,C14,C7,C8)*	6.6	23.3	–	0.0	6.4	7.1	7.3	8.0
r(H/O16,H27)	–	–	–	–	0.967	0.96	0.968	0.968	τ(C13,C14,C7,C12)	173.3	157.2	180.0	180.0	173.8	173.1	173.0	172.3
r(H/O18,H28)	–	–	–	–	0.967	0.968	0.968	0.968	τ(C14,C13,C1,C2)	173.3	157.2	180.0	180.0	173.0	171.3	171.3	169.5
φ(C1,C2,C3)	121.4	-	121.5	121.4	120.3	120.3	120.4	120.	τ(C14,C13,C1,C6)**	6.6	23.3	–	0.0	7.1	8.8	8.8	10.6
φ(C1,C2,H15)	–	–	–	118.9	120.9	120.9	119.	119.6	τ(H25,C13,C1,C2)	–	–	–	0.0	6.0	7.5	7.5	9.1
φ(C1,C6,C5)	120.5	-	121.0	120.9	119.	120.	119.9	120.1	τ(H25,C13,C1,C6)	–	–	–	180.0	173.9	172.4	172.3	170.7
φ(C1,C6,H19)	–	–	–	119.9	121.9	120.5	121.8	120.4	τ(H25,C13,C14,H26)	–	–	–	180.0	177.8	177.3	177.4	176.9
φ(C1,C13,C14)	126.0	126.1	127.5	127.0	126.6	126.7	126.	126.7	τ(H26,C14,C7,C8)	–	–	–	180.0	174.5	174.0	173.8	173.3
φ(C1,C13,H25)	–	–	–	114.2	114.4	114.4	114.6	114.5	τ(H26,C14,C7,C12)	–	–	–	0.0	5.3	5.7	6.0	6.4
φ(C2,C1,C6)	118.1	–	–	117.8	119.3	119.1	119.1	118.8	$\tau^*+\tau^{**}$	13.2	46.6	–	0.0	13.5	15.9	16.1	18.6
φ(C2,C1,C13)	118.8	119.0	118.6	118.7	118.0	118.1	118.1	118.3									

[a] CC: cis-cis; CT: cis-trans; TC: trans-cis; TT: trans-trans. For the numbering of the atoms see Figures 1 and 2. [b] Bond lengths (r) in angstroms, valence (φ) and torsional (τ) angles in degrees. [c] Reference 11, β type molecule. [d] Reference 7. [e] Reference 8. [f] This work.

TABLE 2: Calculated Molecular Energies (Becke3P86/6-31G(d)) of Pinosylvin Conformers

conformer	energies/hartree molecule^{-1} calcd (r_e)	zero point correction	corrected (r_o)	relative r_o energy kJ mol^{-1}	statistical weight/%
cis-cis	−693.155523	0.224215	−692.931308	2.837	2.6
cis-trans	−693.156744	0.224354	−692.932390	0.000	44.4
trans-cis	−693.156616	0.224343	−692.932273	0.306	32.7
trans-trans	−693.156401	0.224308	−692.932093	0.777	20.4

Solid wood samples can be observed most conveniently by the DRIFT method using the FT-IR techniques. Raman spectra were recorded on a Perkin-Elmer System 1760X FT-IR spectrometer equipped with a 1700X Raman accessory. A total of 850 scans were accumulated at a resolution of 1 cm^{-1}. The sample was excited with 0.6 W power from a Spectron SL 301 series Nd:YAG laser intensity stabilized at 1064 nm.

3. Computational Details

Quantum chemical calculations were carried out applying the Gaussian 98 program package with the Becke3P86 DFT functional and the 6-31G(d) basis set.[11] The geometry optimizations providing the molecular energies were followed by frequency calculations using the same basis set. Force constants were calculated by differentiating the molecular potential energy twice with respect to the Cartesian coordinates of the atoms.

TABLE 3: Internal Coordinates and Diagonal Force Constants of trans-Stilbene (TS) and Pinosylvin (PS) Conformers

ser no.	internal coordinate[a]	scale factors TS	PS	TS	diagonal force constants[b] CC PS	CT PS	TC PS	TT PS	ser no.	internal coordinate[a]	scale factors TS	PS	TS	diagonal force constants[b] CC PS	CT PS	TC PS	TT PS
1	$\nu_{1,2}$	0.910	0.932	6.318	6.559	6.652	6.456	6.556	40	$\nu_{7,14}$	0.993	0.932	5.514	5.171	5.170	5.172	5.171
2	$\nu_{2,3}$	0.910	0.932	6.686	6.753	6.650	6.714	6.609	41	$\nu_{12,24}$	0.904	0.917	5.069	5.148	5.142	5.149	5.143
3	$\nu_{3,4}$	0.910	0.932	6.654	6.683	6.798	6.760	6.849	42	$\nu_{11,23}$	0.904	0.917	5.113	5.186	5.186	5.188	5.188
4	$\nu_{4,5}$	0.910	0.932	6.536	6.558	6.638	6.672	6.727	43	$\nu_{10,22}$	0.904	0.917	5.127	5.198	5.199	5.199	5.200
5	$\nu_{5,6}$	0.910	0.932	6.763	6.867	6.824	6.759	6.713	44	$\nu_{9,21}$	0.904	0.917	5.111	5.181	5.183	5.180	5.182
6	$\nu_{6,1}$	0.910	0.932	6.187	6.428	6.336	6.522	6.439	45	$\nu_{8,20}$	0.904	0.917	5.127	5.195	5.197	5.193	5.195
7	$\nu_{1,13}$	0.993	0.932	5.514	5.168	5.173	5.168	5.174	46	$\varphi_{14,8,7}-\varphi_{14,12,7}$	0.993	1.027	1.016	1.040	1.041	1.040	1.038
8	$\nu_{2,15}$	0.904	0.917	5.069	5.246	5.246	5.108	5.107	47	$\varphi_{24,7,12}-\varphi_{24,11,12}$	0.936	0.929	0.522	0.517	0.516	0.517	0.516
9	$\nu_{3,16}$	0.904	0.913	5.113	6.196	6.223	6.198	6.218	48	$\varphi_{23,12,11}-\varphi_{23,10,11}$	0.936	0.929	0.505	0.502	0.502	0.502	0.502
10	$\nu_{4,17}$	0.904	0.917	5.127	5.060	5.190	5.190	5.318	49	$\varphi_{22,11,10}-\varphi_{22,9,10}$	0.936	0.929	0.503	0.499	0.499	0.499	0.500
11	$\nu_{5,18}$	0.904	0.913	5.111	6.181	6.191	6.208	6.211	50	$\varphi_{21,10,9}-\varphi_{21,8,9}$	0.936	0.929	0.509	0.505	0.505	0.505	0.505
12	$\nu_{6,19}$	0.904	0.917	5.127	5.285	5.151	5.285	5.149	51	$\varphi_{20,9,8}-\varphi_{20,7,8}$	0.936	0.929	0.519	0.516	0.516	0.515	0.515
13	$\varphi_{13,6,1}-\varphi_{13,2,1}$	0.993	1.027	1.016	1.050	1.054	1.046	1.046	52	$\varphi_{8,12,7}-\varphi_{7,11,12}+\varphi_{12,10,11}-\varphi_{11,9,10}+\varphi_{10,8,9}-\varphi_{9,7,8}$	0.962	0.963	1.252	1.253	1.253	1.253	1.252
14	$\varphi_{15,1,2}-\varphi_{15,3,2}$	0.936	0.929	0.522	0.486	0.486	0.508	0.509	53	$2\varphi_{8,12,7}-\varphi_{7,11,12}-\varphi_{12,10,11}+2\varphi_{11,9,10}-\varphi_{10,8,9}-\varphi_{9,7,8}$	0.962	0.963	1.299	1.299	1.299	1.299	1.299
15	$\varphi_{16,2,3}-\varphi_{16,4,3}$	0.936	0.971	0.505	0.998	0.997	0.996	0.998	54	$\varphi_{7,11,12}-\varphi_{12,10,11}+\varphi_{10,8,9}-\varphi_{9,7,8}$	0.962	0.963	1.225	1.226	1.227	1.227	1.227
16	$\varphi_{17,3,4}-\varphi_{17,5,4}$	0.936	0.929	0.503	0.496	0.470	0.472	0.447	55	$\theta_{14,8,7,12}$	0.944	0.952	1.660	1.649	1.661	1.659	1.666
17	$\varphi_{18,4,5}-\varphi_{18,6,5}$	0.936	0.971	0.509	1.006	1.008	1.005	1.009	56	$\theta_{24,7,12,11}$	0.982	0.948	1.605	1.559	1.554	1.561	1.554
18	$\varphi_{19,5,6}-\varphi_{19,1,6}$	0.936	0.929	0.519	0.485	0.507	0.485	0.508	57	$\theta_{23,12,11,10}$	0.982	0.948	1.813	1.747	1.747	1.749	1.749
19	$\varphi_{6,2,1}-\varphi_{1,3,2}+\varphi_{2,4,3}-\varphi_{3,5,4}+\varphi_{4,6,5}-\varphi_{5,1,6}$	0.962	0.963	1.252	1.279	1.279	1.279	1.279	58	$\theta_{22,11,10,9}$	0.982	0.948	1.756	1.702	1.704	1.704	1.705
20	$2\varphi_{6,2,1}-\varphi_{1,3,2}-\varphi_{2,4,3}+2\varphi_{3,5,4}-\varphi_{4,6,5}-\varphi_{5,1,6}$	0.962	0.963	1.299	1.282	1.277	1.277	1.272	59	$\theta_{21,10,9,8}$	0.982	0.948	1.793	1.738	1.739	1.737	1.738
21	$\varphi_{1,3,2}-\varphi_{2,4,3}+\varphi_{4,6,5}-\varphi_{5,1,6}$	0.962	0.963	1.225	1.298	1.304	1.304	1.308	60	$\theta_{20,9,8,7}$	0.982	0.948	1.697	1.644	1.646	1.641	1.644
22	$\theta_{13,6,1,2}$	0.944	0.952	1.660	1.653	1.649	1.656	1.652	61	$\tau_{8,7,12,11}-\tau_{7,12,11,10}+\tau_{12,11,10,9}-\tau_{11,10,9,8}+\tau_{10,9,8,7}-\tau_{9,8,7,12}$	0.975	0.952	0.381	0.372	0.372	0.372	0.372
23	$\theta_{15,1,2,3}$	0.982	0.948	1.740	1.476	1.483	1.334	1.342	62	$\tau_{9,8,7,12}-\tau_{8,7,12,11}+\tau_{12,11,10,9}-\tau_{11,10,9,8}$	0.975	0.952	0.300	0.294	0.294	0.294	0.294
24	$\theta_{16,2,3,4}$	0.982	0.918	1.813	2.228	2.241	1.900	1.902	63	$\tau_{8,24,12,11}-2\tau_{7,12,11,10}+\tau_{12,11,10,9}+\tau_{11,10,9,8}-2\tau_{10,9,8,7}+\tau_{9,8,7,12}$	0.975	0.952	0.322	0.315	0.315	0.315	0.315
25	$\theta_{17,3,4,5}$	0.982	0.948	1.756	1.180	1.320	1.347	1.466	64	$\nu_{26,14}$	0.904	0.917	5.010	5.090	5.075	5.093	5.078
26	$\theta_{18,4,5,6}$	0.982	0.918	1.793	2.124	2.012	2.142	2.015	65	$\varphi_{26,7,14}$	0.936	0.929	1.109	1.096	1.094	1.094	1.092
27	$\theta_{19,5,6,1}$	0.982	0.948	1.697	1.465	1.294	1.469	1.300	66	$\tau_{26,14,7,12}$	0.978	0.948	0.026	0.034	0.037	0.037	0.040
28	$\tau_{6,1,2,3}-\tau_{1,2,3,4}+\tau_{2,3,4,5}-\tau_{3,4,5,6}+\tau_{4,5,6,1}-\tau_{5,6,1,2}$	0.975	0.952	0.381	0.330	0.329	0.329	0.328	67	$\nu_{13,14}$	0.876	0.932	8.008	8.536	8.529	8.533	8.525
29	$\tau_{5,6,1,2}-\tau_{6,1,2,3}+\tau_{2,3,4,5}-\tau_{3,4,5,6}$	0.975	0.952	0.300	0.297	0.308	0.307	0.318	68	$\varphi_{13,7,14}$	1.003	1.027	1.648	1.643	1.647	1.643	1.646
30	$\tau_{6,1,2,3}-2\tau_{1,2,3,4}+\tau_{2,3,4,5}+\tau_{3,4,5,6}-2\tau_{4,5,6,1}+\tau_{5,6,1,2}$	0.975	0.952	0.324	0.307	0.298	0.298	0.286	69	$\varphi_{14,1,13,0}$	1.003	1.027	1.648	1.656	1.667	1.654	1.660
31	$\nu_{25,13}$	0.904	0.917	5.010	5.098	5.103	5.085	5.089	70	$\tau_{1,13,14,7}$	1.020	0.952	0.444	0.415	0.414	0.419	0.418
32	$\varphi_{25,1,13}$	0.936	0.929	1.109	1.092	1.091	1.092	1.091	71	$\theta_{13,7,14,26}$	0.982	0.948	1.102	1.111	1.116	1.129	1.130
33	$\tau_{25,13,1,2}$	0.978	0.948	0.026	0.032	0.039	0.036	0.043	72	$\theta_{14,1,13,25}$	0.982	0.948	1.102	1.092	1.117	1.109	1.134
34	$\nu_{7,12}$	0.910	0.932	6.318	6.473	6.473	6.473	6.472	73	$\nu_{27,16}$		0.804		6.478	6.470	6.475	6.476
35	$\nu_{12,11}$	0.910	0.932	6.686	6.832	6.836	6.835	6.838	74	$\varphi_{27,3,16}$		0.952		0.792	0.796	0.796	0.797
36	$\nu_{11,10}$	0.910	0.932	6.654	6.810	6.810	6.810	6.809	75	$\tau_{27,16,3,4}$		0.985		0.055	0.063	0.063	0.063
37	$\nu_{10,9}$	0.910	0.932	6.536	6.688	6.691	6.690	6.692	76	$\nu_{28,18}$		0.804		6.488	6.472	6.480	6.474
38	$\nu_{9,8}$	0.910	0.932	6.763	6.927	6.926	6.926	6.925	77	$\varphi_{28,5,18,}$		0.952		0.793	0.794	0.797	0.796
39	$\nu_{8,7}$	0.910	0.932	6.187	6.342	6.345	6.344	6.346	78	$\tau_{28,18,5,4}$		0.985		0.055	0.065	0.063	0.064

[a] For numbering of the atoms see Figures 1 and 2. [b] CC:cis-cis, CT:cis−trans, TC:trans-cis, TT:trans-trans; units: 10^2 N m^{-1} and 10^{-18} N m, respectively.

TABLE 4: Calculated Atomic Net Charges of trans-Stilbene (TS) and the Pinosylvin (PS) Conformers[a]

atom[b]	TS	CC PS	CT PS	TC PS	TT PS
C1	0.158	0.155	0.154	0.157	0.158
C2	−0.222	−0.272	−0.271	−0.307	−0.307
C3	−0.164	0.362	0.360	0.359	0.359
C4	−0.162	−0.313	−0.276	−0.277	−0.237
C5	−0.166	0.363	0.361	0.361	0.361
C6	−0.200	−0.254	−0.287	−0.254	−0.289
C7	0.158	0.156	0.157	0.156	0.157
C8	−0.200	−0.200	−0.200	−0.200	−0.200
C9	−0.166	−0.167	−0.166	−0.166	−0.166
C10	−0.162	−0.162	−0.162	−0.161	−0.162
C11	−0.164	−0.165	−0.165	−0.165	−0.164
C12	−0.222	−0.221	−0.221	−0.221	−0.221
C13	−0.208	−0.212	−0.209	−0.212	−0.210
C14	−0.208	−0.206	−0.207	−0.205	−0.206
H15	0.160	0.169	0.170	0.145	0.145
H/O16	0.164	−0.658	−0.658	−0.661	−0.658
H17	0.163	0.138	0.164	0.164	0.187
H/O18	0.164	−0.658	−0.661	−0.658	−0.658
H19	0.160	0.170	0.145	0.170	0.145
H20	0.160	0.162	0.162	0.159	0.160
H21	0.164	0.164	0.165	0.163	0.165
H22	0.163	0.163	0.164	0.164	0.164
H23	0.164	0.164	0.164	0.165	0.165
H24	0.160	0.161	0.158	0.162	0.159
H25	0.154	0.157	0.159	0.152	0.155
H26	0.154	0.159	0.151	0.160	0.153
H27	-	0.423	0.425	0.425	0.424
H28	-	0.422	0.425	0.425	0.424

[a] CC: cis-cis, CT: cis−trans, TC: trans-cis, TT: trans-trans; atomic charge units. [b] For the numbering of the atoms see Figures 1 and 2.

Harmonic vibrational frequencies and IR intensities were calculated, too.

The calculated geometry and the force field were applied to the further force field refinement in internal coordinate representation and for fitting the calculated frequencies to the experimental ones. The potential energy distribution (PED) matrix elements were calculated from these results. The normal coordinate calculations were carried out with our own computer programs.

4. Results and Discussion

Four conformers of the PS molecule were investigated during the calculations, depending on the positions of the atoms H_{27} and H_{28}. The positions of these atoms are denoted cis (C) and trans (T), if they are in cis position and trans position with respect to C_4, respectively. The individual conformers are labeled by two letters: the first one refers to the position of atom H_{27}, while second one refers to the that of atom H_{28}. Figure 1 illustrates trans-trans-pinosylvin. The results for pinosylvin were compared with the corresponding data of trans-stilbene.

A. Geometric Parameters. The calculated equilibrium (r_e) geometric parameters of the TS and PS conformers are listed in Table 1. The geometric parameters of the trans-stilbene molecule were measured with X-ray diffraction by Hoekstra et al.[12] They investigated the crystal structure of the molecule in the crystal and found two different forms, α and β. According to their results, both molecules have nonplanar structure. Since the β type molecules are more distant from each other in the crystal, Table 1 introduces this geometry. For this molecule the angle between the planes of the two benzene rings ($\tau^*+\tau^{**}$) was 13.2°.

The quantum chemical calculations with RHF/6-31G(d)[5] seem to support the experimental data, which resulted in 23.3 degrees between the two benzene rings. However, both Negri's[9] and

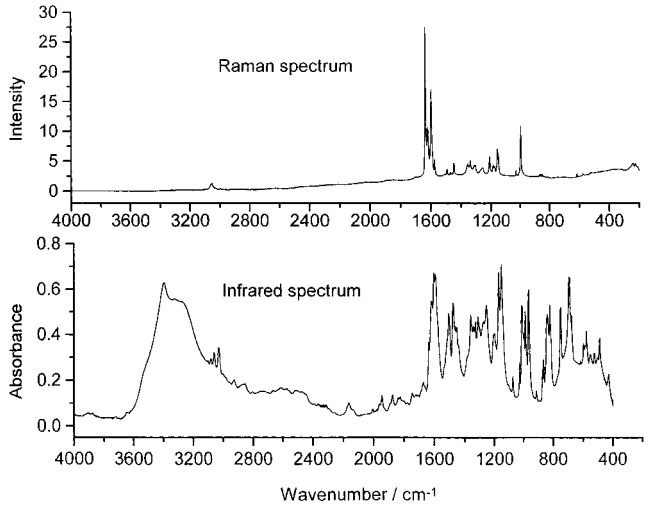

Figure 3. Measured infrared and Raman spectra of pinosylvin.

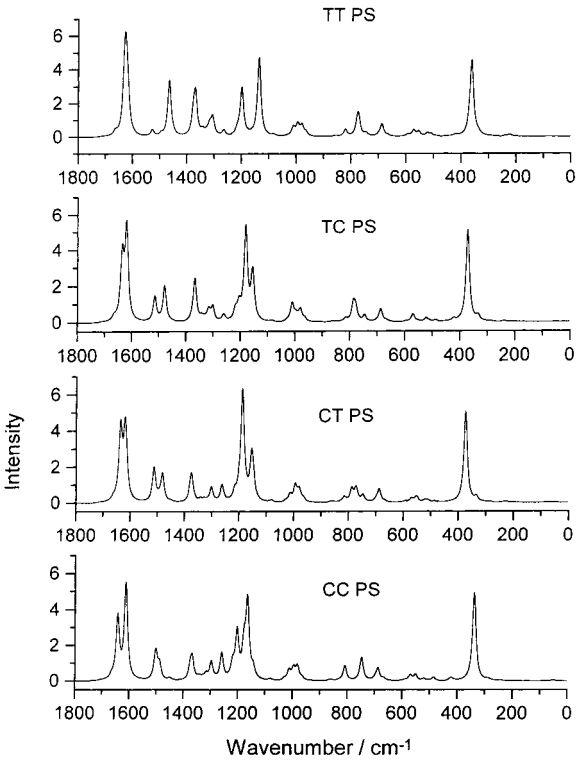

Figure 4. Simulated infrared spectra of the four pinosylvin conformers in the 1800−0 cm^{-1} region (see text for details).

our post-Hartree−Fock DFT calculations, BLYP/6-31G(d) and B3P86/6-31G(d), resulted in planar structures with C_{2h} symmetry. In our opinion the crystalline and isolated structures of the TS molecule can substantially differ from each other since their environments are very different. Therefore Negri's and our results are possibly not in contradiction with the experimental data. The extended conjugation between the two rings through the vinylidene group makes the planarity of the isolated molecule considerably probable.

Regarding the investigated four pinosylvin conformers, the most important effect is the influence of the two hydroxyl groups on the molecular structure. Comparing the results of our calculations on TS and the PS conformers, one can state the following: (a) the molecule is no longer planar; (b) the bond lengths of the TS molecule do not change significantly on substitution; (c) the changes of atoms 16 and 18 from hydrogen to oxygen cause changes in the angles between the substituent

TABLE 5: Vibrational Frequencies and Potential Energy Distributions of trans-Stilbene[a]

wavenumber/cm^{-1}										wavenumber/cm^{-1}									
meas.[c]	calc.	PED/%[b] (distributions ≥ 10%)								meas.[c]	calc.	PED/%[b] (distributions ≥ 10%)							
3079	3069	νCHr	99							1026	1020	νrg	70	βCHr	21				
3079	3069	νCHr	99							1002	988	νrg	31	βrg	67				
3061	3060	νCHr	99							997	1000	γCHr	31	γCHv	57				
3059	3060	νCHr	99							995	987	νrg	36	βrg	62				
3054	3051	νCHr	99							985	979	γCHr	63	γCHv	22				
3053	3052	νCHr	99							984	986	γCHr	82						
3038	3042	νCHr	99							969	957	γCHr	89						
3036	3043	νCHr	98							947	956	γCHr	94						
3028	3034	νCHr	99							915	919	γCHr	67	γCHv	14				
3028	3034	νCHr	98							910	909	γCHr	83						
3014	3020	νCHv	97							869	871	γCHr	37	γCHv	58				
3004	3013	νCHv	97							866	868	νrg	38	βrg	15	βCC	25		
1639	1639	νCC	62	βCHv	25					853	839	γCHr	89						
1599	1614	νrg	65	βrg	10	βCHr	20			847	841	γCHr	99						
1594	1605	νrg	63	βrg	10	βCHr	21			823	819	νrg	47	νCC	23	βrg	26		
1578	1585	νrg	66	βCHr	18					764	772	τrg	27	τCC	26	γCHr	44		
1571	1579	νrg	63	βCHr	19					738	743	τrg	15	γCHr	67				
1496	1500	νrg	34	βCHr	55					693	697	τrg	68	γCHr	30				
1490	1488	νrg	33	βCHr	60					688	692	τrg	92						
1452	1450	νrg	36	βCHr	50					640	640	βrg	64	βCC	18				
1445	1443	νrg	37	βCHr	54					616	617	νrg	10	βrg	86				
1339	1331	νrg	43	βCHr	48					616	620	νrg	10	βrg	84				
1332	1323	νrg	36	νCC	14	βCHr	15	βCHv	31	541	539	βrg	81						
1332	1345	νrg	41	βCHr	13	βCHv	34			527	535	τrg	48	τCC	49				
1326	1328	νrg	23	βCHr	70					469	465	τrg	57	τCC	34				
1318	1312	νCC	14	βCC	28	βCHr	30	βCHv	18	464	468	νrg	10	βCC	82				
1308	1287	νrg	26	νCC	37	βCHr	27			410	405	τrg	92						
1221	1226	νrg	26	βCHr	17	βCHv	47			407	407	τrg	93						
1192	1199	νrg	26	νCC	32	βrg	12	βCHr	20	290	286	τrg	72	τCC	22				
1182	1175	νrg	24	βCHr	74					289	284	νrg	10	νCC	24	βrg	17	βCC	47
1160	1172	νrg	22	βCHr	74					227	218	τrg	47	τCC	36	γCHv	13		
1156	1151	νrg	17	βCHr	82					204	204	νCC	16	βrg	13	βCC	63		
1155	1150	νrg	17	βCHr	82					81	81	βCC	97						
1074	1077	νrg	53	βCHr	40					66	66	τrg	13	γCHv	85				
1073	1074	νrg	54	βCHr	38					60	60	τCC	88						
1030	1022	νrg	71	βCHr	23					7	7	γCHv	98						

[a] Mean deviation 5.44 cm^{-1}; mean relative devation 0.59% [b] ν: stretching, β: in-plane deformation, γ: out-of-plane deformation, τ: torsion, CC: at least one carbon atom does not belong to ring; v: vinylidene group; r, rg: ring. [c] wavenumbers below 200 cm^{-1} are chosen as equal to the calculated ones.

bonds and the ring bonds in the substituted ring, and this is true not only for the C−O but also for the C−H bonds (H atoms 15, 17 and 19).

The effect on conformational change is observable from the values of torsional angles $C_4C_3O_{16}H_{27}$ and $C_4C_5O_{18}H_{28}$ characterizing both the conformer and the coplanarity of the OH groups and the benzene ring. The slight deviations from 0 and 180 degrees are smaller than the errors in the calculations. The substitution has only a minor influence on the structure of the benzene rings and the vinylidene group. However, the angle between the planes of the two benzene rings (Table 1, τ *+τ **) increases from the cis-cis (CC) conformer to the trans-trans (TT) one. For the cis-trans (CT) and trans-cis (TC) conformers, these angles are nearly equal. A smaller effect of the conformation change can be observed on the OCC angles and the HCC angles of the substituted ring.

B. Molecular Energy. Table 2 summarizes the calculated molecular energies of the four PS conformers as isolated molecules. Both the equilibrium (r_e) and the zero-point corrected energies show that the CT conformer has the lowest energy (see Table 2). The CC conformer has the highest energy; the difference to the CT conformer is almost 3 kJ mol^{-1}. The energy differences to the TC and TT conformers are less than 1 kJ mol^{-1}. Consequently, the statistical weights of the CT, TC, and TT conformers are considerable in the mixture.

C. Vibrational Force Constants. The pinosylvin molecule (Figure 1) consists of 28 atoms, i.e., it has 78 vibrational modes. According to its structure it has no symmetry elements, i.e., it belongs to the general C_1 point group.

The output file of the quantum chemical calculations contains the vibrational force constants in a Cartesian coordinate system and in quantum mechanical units: hartree bohr^{-2}. These force constants were transformed into chemical internal coordinates (Table 3) and into SI units. The next step was fit to the calculated force constants to the experimental frequencies. The force constants of the most probable CT conformer were used for this procedure. The scaling was carried out with a homemade computer program applying the method of weighted least squares. The scale factors yielded are also presented in Table 3. The values of the scale factors are between 0.9 and 1.0 in most of the cases, with one important exception: the scale factors for the OH stretching force constants are very low. This is the consequence of fitting the calculated OH stretching frequencies to the experimental values. The very strong association shifted this band to lower frequencies. The frequencies of the isolated molecule are unknown, thus we decided to base the scaling procedure on the observed values. The scale factors calculated in this way were applied to the scaling of the other three conformers. Since the number of independent force

TABLE 6: Vibrational Frequencies and Potential Energy Distributions of cis-cis Pinosylvin[a]

wavenumber/cm^{-1}				wavenumber/cm^{-1}			
meas.[c]	calc.	PED/%[b] (distributions ≥ 10%)		meas.[c]	calc.	PED/%[b] (distributions ≥ 10%)	
3405	3405	νOH 99	O18−H28 stretching	995	991	νrg 36 βrg 56	
3397	3402	νOH 99	O16−H27 stretching	987	985	νrg 41 βrg 46	
3103	3103	νCHr 99	C6−H19 stretching	979	981	γCHr 21 γCHv 66	
3103	3092	νCHr 99	C2−H15 stretching	964	964	γCHr 70 γCHv 14	
3082	3090	νCHr 99	unsubstituted ring stretching	914	940	γCHr 97	
3082	3081	νCHr 98	unsubstituted ring stretching	909	902	γCHr 69 γCHv 11	
3060	3073	νCHr 99	unsubstituted ring stretching	864	865	γCHr 32 γCHv 52	
3060	3064	νCHr 98	unsubstituted ring stretching	851	853	νrg 34 νCCv 13 βrg 18 βCCv 18	
3056	3057	νCHr 99	unsubstituted ring stretching	829	828	γCHr 97	
3056	3046	νCHv 97	anti-phase stretching	819	821	γCHr 73 γCO 10	
3029	3039	νCHv 97	in-phase stretching	771	808	γCHr 66	
3029	3035	νCHr 99	C4−H17 stretching	751	750	τrg 10 γCCv 14 γCHr 61 γCO 10	
1674	1664	νrg 13	νCCv 60 βCHv 19	746	747	γCHr 76 γCO 13	
1637	1642	νrg 61		693	699	νrg 20 βrg 36 βCCv 18	
1618	1619	νrg 66	βCHr 19	688	688	τrg 68 γCHr 28	
1601	1612	νrg 62	βCHr 16	675	667	τrg 82	
1588	1594	νrg 66	βCHr 17	619	620	νrg 10 βrg 84	
1516	1502	νrg 41	βCHr 25 βOH 11	597	593	τrg 17 γCO 75	
1494	1497	νrg 38	βCHr 41	585	591	τrg 23 γCCv 38 γCO 30	
1472	1487	νrg 39	βCHr 35 βOH 10	578	570	νrg 18 νCO 12 βrg 48	
1448	1451	νrg 39	βCHr 49	551	551	βrg 10 βCCv 35 βCO 44	
1363	1374	νrg 54	νCO 10 βCHv 11	522	521	νrg 10 βrg 76	
1358	1367	νrg 39	νCCv 10 νCO 28 βrg 10	499	513	βrg 79	
1341	1341	νrg 76	βCHr 14	487	486	τrg 50 γCCv 39	
1328	1328	νCCv 19	βCCv 13 βCHr 13 βCHv 51	427	422	νrg 11 βCCv 55 βCO 24	
1314	1316	βCCv 10	βCHr 61 βCHv 17	401	401	τrg 99	
1306	1298	νrg 12	βCHr 53 βOH 13	376	340	τOH 93	
1256	1259	νrg 17	νCCv 17 βCHr 21 βCHv 20 βOH 11	360	339	τOH 94	
1210	1219	νrg 19	νCCv 11 βCHr 10 βCHv 25 βOH 31	334	334	νrg 11 βrg 10 βCO 68	
1201	1203	νrg 21	νCCv 13 βCHr 11 βOH 38	288	286	τrg 61 γCCv 24	
1187	1178	νCO 38	βCHr 52	247	242	νrg 12 νCCv 19 βCCv 29 βCO 10 τrg 14	
1177	1173	νrg 21	βCHr 74	238	237	τrg 68	
1170	1165	νrg 22	βCHr 30 βOH 40	222	225	τrg 79 γCO 10	
1157	1149	νrg 15	βCHr 83	205	201	τrg 39 γCCv 26 γCO 23	
1150	1143	νrg 12	νCCv 20 βCHr 50	178	179	νCCv 13 βCCv 61	
1074	1081	νrg 51	βCHr 42	84	80	βCCv 31 γCHv 55	
1028	1029	νrg 71	βCHr 23	57	58	βCCv 62 γCHv 23	
1007	1012	νrg 44	νCO 23 βCHr 14	51	50	τrg 10 γCCv 84	
999	996	νrg 39	νCCv 11 νCO 10 βrg 23	14	11	γCHv 97	

[a] Mean deviation 5.86 cm^{-1}. Mean relative deviation 1.06%. [b] ν: stretching, β: in-plane deformation, γ: out-of-plane deformation, τ: torsion, CC: at least one carbon atom does not belong to ring; v: vinylidene group; r, rg: ring. [c] Wavenumbers below 200 cm^{-1} are chosen as equal to the for CT calculated ones.

constants is very large, only the diagonal F matrix elements are listed in Table 3.

Similarly to the PS conformers, the TS force constants were also subjected to a scaling procedure. The chemical internal coordinates are the same in both cases, TS differs only in the number of atoms (26) and consequently the vibrational modes (72) since TS contains only H atoms instead of the OH groups. The yielded scale factors and diagonal force constants are included in Table 3.

The effect of the conformation change is interesting first of all with respect to the OH-substituted ring of PS. Here one expects the sum of the electron repulsive effects of the two OH groups on one another, on all carbon atoms in this ring, and on the vinylidene group. By examining the conformation effect on the diagonal force constants of stretching coordinates of this ring, the following can be observed. With respect to the CC conformer, the change from CC to TT conformer increases the force constants of the bonds between C3−C4 and C4−C5, whereas the force constants of the other two bonds near the OH groups C2−C3 and C5−C6 decrease even when only one OH group changes to trans. The remaining two ring stretching force constants (those of C1−C2 and C6−C1) decrease if the OH group next to the bond is in trans position, and they increase if this group is in cis position. For the TT conformation both constants remain unchanged. The trans conformation of one of the OH groups increases the diagonal stretching force constant of the other OH group. The influence of the conformation on the C−O and C−H diagonal stretching force constants of this ring is negligible. The importance and influence of the conformation change in other parts of the molecule is also negligible as a consequence of the nonplanarity of the two rings that leads to decreasing of the conjugation with the vinylidene group.

D. Atomic Net Charges. Table 4 contains the calculated atomic net charges for trans-stilbene and for pinosylvin conformers. The information that they represent is in good accordance with that of the vibrational force constants. Comparing the data of TS and PS, the net charges of the unsubstituted ring and the vinylidene group are independent of the substitution of the two OH groups. On the other ring, the carbon atoms in ortho and para positions to the vinylidene group became more negative, while those in the meta position (with the OH substitution) changed their negative net charge to positive.

The conformation changes of PS influence the net charges of the ortho (C2 and C6) and para (C4) atoms and their adjacent hydrogens. Regarding again the CC conformer as a basis, a change of the conformation of the first OH group (on C3) from cis to trans causes C2 and the adjacent H15 to become more

TABLE 7: Vibrational Frequencies and Potential Energy Distributions of cis−trans Pinosylvin[a]

wavenumber/cm^{-1}												wavenumber/cm^{-1}										
meas.[c]	calc.	PED/%[b] (distributions ≥ 10%)										meas.[c]	calc.	PED/%[b] (distributions ≥ 10%)								
3405	3401	νOH	99					O18−H28 stretching				999	994	νrg	34	βrg	32					
3397	3400	νOH	99					O16−H27 stretching				995	990	νrg	40	βrg	40					
3103	3092	νCHr	99					C2−H15 stretching				987	987	νrg	43	βrg	53					
3103	3090	νCHr	99					unsubstituted ring stretching				979	979	γCHr	26	γCHv	62					
3082	3081	νCHr	98					unsubstituted ring stretching				964	964	γCHr	67	γCHv	17					
3082	3076	νCHr	99					C4−H17 stretching				914	940	γCHr	97							
3060	3073	νCHr	99					unsubstituted ring stretching				909	902	γCHr	70	γCHv	11					
3060	3064	νCHr	98					unsubstituted ring stretching				864	865	γCHr	31	γCHv	50					
3056	3062	νCHr	97					unsubstituted ring stretching				851	853	νrg	34	νCCv	13	βrg	18	βCCv	17
3056	3056	νCHr	99					C6−H19 stretching				829	828	γCHr	97							
3029	3046	νCHv	97					anti-phase stretching				819	815	γCHr	69	γCHv	10					
3029	3035	νCHv	97					in-phase stretching				771	788	γCHr	70	γCO	14					
1674	1663	νCCv	63	βCHv	20							751	772	γCCv	10	γCHr	68					
1637	1636	νrg	66									746	747	τrg	21	γCCv	15	γCHr	55			
1618	1621	νrg	67	βCHr	17							693	699	νrg	20	βrg	36	βCCv	18			
1601	1617	νrg	61	βCHr	15							688	688	τrg	69	γCHr	27					
1588	1594	νrg	66	βCHr	17							675	668	τrg	84							
1516	1512	νrg	39	βCHr	28	βOH	12					619	620	νrg	10	βrg	84					
1494	1494	νrg	36	βCHr	54							597	596	τrg	16	γCO	74					
1472	1481	νrg	44	βCHr	19	βOH	11					585	593	τrg	24	γCCv	40	γCO	29			
1448	1451	νrg	39	βCHr	49							578	570	νrg	19	νCO	13	βrg	46			
1363	1376	νrg	66	βCHv	10	βOH	13					551	552	βrg	13	βCCv	34	βCO	41			
1358	1371	νrg	23	νCCv	16	νCO	34	βrg	14			522	522	νrg	10	βrg	77					
1341	1342	νrg	77	βCHr	13							499	511	βrg	77							
1328	1327	νCCv	18	βCCv	12	βCHr	16	βCHv	50			487	487	τrg	50	γCCv	39					
1314	1316	βCCv	10	βCHr	59	βCHv	19					427	422	νrg	11	βCCv	55	βCO	23			
1306	1301	νrg	12	βCHr	53	βOH	16					401	401	τrg	99							
1256	1262	νrg	17	νCCv	18	βCHr	18	βCHv	24			376	375	τOH	96							
1210	1216	νrg	20	νCCv	13	βCHr	16	βCHv	26	βOH	18	360	361	τOH	95							
1201	1201	νrg	17	βCHr	19	βOH	41					334	335	νrg	12	βrg	10	βCO	69			
1187	1188	νrg	18	νCO	17	βCHr	21	βOH	32			288	288	τrg	59	γCCv	24					
1177	1173	νrg	20	βCHr	75							247	243	νrg	10	νCCv	16	βCCv	24	τrg	25
1170	1154	νCO	23	βCHr	47	βOH	18					238	238	τrg	60							
1157	1149	νrg	15	βCHr	80							222	224	τrg	78							
1150	1147	νrg	13	νCCv	15	βCHr	56					205	202	τrg	40	γCCv	25	γCO	23			
1074	1081	νrg	51	βCHr	42							178	178	νCCv	13	βCCv	60					
1028	1029	νrg	71	βCHr	23							84	84	βCCv	28	γCHv	57					
1007	1014	νrg	44	νCO	20	βCHr	14					57	57	βCCv	65	γCHv	21					
												51	51	γCCv	85							
												14	14	γCHv	97							

[a] Mean deviation 4.99 cm−1. Mean relative deviation 0.53%. [b] ν: stretching, β: in-plane deformation, γ: out-of-plane deformation, τ: torsion, CC: at least one carbon atom does not belong to ring; v: vinylidene group; r, rg: ring. [c] Wavenumbers below 200 cm^{-1} are chosen as equal to the calculated ones.

negative and the C2−H15 bond more polar. If the second OH group (on C5) similarly changes its conformation, the same effect is observed on C6 and H19, and on the corresponding C6−H19 bond. A reversed effect is observed on C4 and H17: if any of the OH groups changes its conformation, both atoms become more positive and the C4−H17 bond less polar. Both atoms have their most positive charges when both OH groups have trans conformation. The net charges of all other atoms in the molecule remain practically constant.

Summing it up, the cis to trans change in the conformation of the OH groups produces electron repulsion of the atoms H17 and C4 in the direction of the vinylidene group.

E. Vibrational Frequencies and Spectra. The recorded vibrational spectra of pinosylvin are presented in Figure 3. The spectra were analyzed by curve fit of the overlapping bands. The very strong association as a result of the H−O···H type hydrogen bonds is striking in the infrared spectrum but hardly observable in the Raman spectrum.

The results of the normal coordinate analyses are presented in Table 5 (trans-stilbene), 6 (cis-cis), 7 (cis-trans), 8 (trans-cis), and 9 (trans-trans). The tables contain the experimental fundamentals between 4000 and 200 cm^{-1}. The figures found in these columns below 200 cm^{-1} are the scaled calculated fundamentals for TS (Table 5) and cis-trans PS (Tables 6−9). The force constants calculated for the cis-trans conformer were scaled to fit the measured spectrum, and these scale factors were also applied in the case of the other conformers.

The most characteristic vibrational modes are CH stretchings for both TS and PS and OH stretchings for PS. The ten CH stretching modes of TS are coupled not only within each ring but also between the stretching coordinates of the two benzene rings. The CH stretching modes of PS are very different. The two rings are not coplanar anymore. On the substituted ring, the OH groups are placed between the CH groups. Therefore coupling between the CH stretchings of the two rings and also between these groups of the substituted ring are not possible. The decoupling of the OH stretching vibration has similar reasons. As noted in Tables 6−9, the CH stretches of the nonsubstituted ring are coupled, while those of the substituted one appear as characteristic CH vibrations for each CH group. The order of their wavenumbers depends on their conformation as follows. For the cis-cis conformer: $\nu(C_6H_{19}) > \nu(C_2H_{15}) > \nu(C_4H_{17})$. For the cis-trans conformer: $\nu(C_2H_{15}) > \nu(C_4H_{17}) > \nu(C_6H_{19})$. For the trans-cis conformer: $\nu(C_6H_{19}) > \nu(C_4H_{17}) > \nu(C_2H_{15})$. For the trans-trans conformer: $\nu(C_4H_{17}) > \nu(C_6H_{19}) > \nu(C_2H_{15})$.

TABLE 8: Vibrational Frequencies and Potential Energy Distribution of trans-cis Pinosylvin[a]

wavenumber/cm^{-1}										wavenumber/cm^{-1}											
meas.[c]	calc.	PED/%[b] (distributions ≥ 10%)								meas.[c]	calc.	PED/%[b] (distributions ≥ 10%)									
3405	3403	νOH	99	O18−H28 stretching						995	991	νrg	36	βrg	56						
3397	3401	νOH	99	O16−H27 stretching						987	987	νrg	41	βrg	51						
3103	3103	νCHr	99	C6−H19 stretching						979	980	γCHr	24	γCHv	63						
3103	3090	νCHr	99	unsubstituted ring stretching						964	964	γCHr	68	γCHv	16						
3082	3081	νCHr	99	unsubstituted ring stretching						914	940	γCHr	97								
3082	3075	νCHr	99	C4−H17 stretching						909	902	γCHr	70	γCHv	10						
3060	3073	νCHr	99	unsubstituted ring stretching						864	862	γCHr	24	γCHv	59						
3060	3063	νCHr	99	unsubstituted ring stretching						851	853	νrg	33	νCCv	13	βrg	17	βCCv	17		
3056	3057	νCHr	99	unsubstituted ring stretching						829	827	γCHr	96								
3056	3050	νCHr	96	C2−H15 stretching						819	815	γCHr	74								
3029	3044	νCHv	96	anti-phase stretching						771	787	γCHr	67	γCO	16						
3029	3037	νCHv	97	in-phase stretching						751	778	γCCv	11	γCHr	72						
1674	1664	νrg	13	νCCv	59	βCHv	19			746	746	τrg	19	γCCv	13	γCHr	57				
1637	1635	νrg	60							693	698	νrg	20	βrg	35	βCCv	19				
1618	1619	νrg	62	βCHr	16					688	688	τrg	69	γCHr	27						
1601	1619	νrg	67	βCHr	15					675	668	τrg	85								
1588	1594	νrg	67	βCHr	17					619	620	νrg	10	βrg	84						
1516	1514	νrg	39	βCHr	27	βOH	12			597	596	τrg	15	γCO	76						
1494	1495	νrg	36	βCHr	55					585	593	τrg	24	γCCv	40	γCO	29				
1472	1478	νrg	42	νCO	10	βCHr	19	βOH	12	578	570	νrg	18	νCO	12	βrg	47				
1448	1451	νrg	39	βCHr	48					551	552	βrg	12	βCCv	34	βCO	41				
1363	1376	νrg	55	βCHv	11	βOH	13			522	522	νrg	10	βrg	77						
1358	1367	νrg	39	νCCv	12	νCO	30	βrg	11	499	511	βrg	77								
1341	1341	νrg	75	βCHr	15					487	487	τrg	50	γCCv	39						
1328	1328	νCCv	20	βCCv	13	βCHr	10	βCHv	52	427	422	νrg	11	βCCv	55	βCO	23				
1314	1316	βCHr	65	βCHv	14					401	401	τrg	99								
1306	1301	νrg	11	βCHr	54	βOH	18			376	372	τOH	97								
1256	1261	νrg	18	νCCv	17	βCHr	16	βCHv	26	360	358	τOH	96								
1210	1218	νrg	19	νCCv	14	βCHv	21	βOH	28	334	334	νrg	12	βrg	10	βCO	69				
1201	1205	νrg	19	βCHr	16	βOH	37			288	288	τrg	59	gCCv	24						
1187	1181	νrg	18	νCO	17	βCHr	32	βOH	25	247	242	νrg	11	νCCv	17	βCCv	25	τrg	23		
1177	1173	νrg	21	βCHr	75					238	237	τrg	64								
1170	1156	νrg	10	νCO	17	βCHr	49	βOH	17	222	224	τrg	76	γCO	10						
1157	1152	νrg	12	νCCv	15	νCO	11	βCHr	50	205	202	τrg	40	γCCv	25	γCO	23				
1150	1149	νrg	14	βCHr	81					178	178	νCCv	13	βCCv	60						
1074	1081	νrg	51	βCHr	42					84	83	βCCv	29	γCHv	57						
1028	1029	νrg	71	βCHr	23					57	57	βCCv	65	γCHv	21						
1007	1010	νrg	44	νCO	19	βCHr	16			51	51	γCCv	85								
999	996	νrg	38	νCCv	12	νCO	12	βrg	19	14	14	γCHv	97								

[a] Mean deviation 4.85 cm^{-1}. Mean relative deviation 0.55%. [b] ν: stretching, β: in-plane deformation, γ: out-of-plane deformation, τ: torsion, CC: at least one carbon atom does not belong to ring; v: vinylidene group; r, rg: ring. [c] Wavenumbers below 200 cm^{-1} are chosen as equal to the for CT calculated ones.

Table 10 is an extract from Tables 6−9 to summarize the positions of the OH and CH stretching modes on the substituted ring. The shift of the CH stretching modes is clear from the figures. If the OH group on C_5 turns from cis to trans (the other OH group remains in cis position), $\nu(C_2H_{15})$ does not change, $\nu(C_4H_{17})$ increases, and $\nu(C_6H_{19})$ decreases. If the OH group on C_3 turns from cis to trans (the other OH group remains in cis position), $\nu(C_6H_{19})$ does not change, $\nu(C_4H_{17})$ increases and $\nu(C_2H_{15})$ decreases. If both OH groups turn from cis to trans positions, $\nu(C_2H_{15})$ and $\nu(C_6H_{19})$ preserve, or nearly preserve, their positions obtained in the cis-trans and trans-cis conformations, respectively, while $\nu(C_4H_{17})$ further increases. The tendencies are very similar to those mentioned in section 4D about the electron repulsion as a consequence of the change in conformation. The conformation effect is considerably smaller on the νOH stretching modes. As long as one of the OH groups is in the cis position, $\nu(O_{18}H_{28})$ is higher than $\nu(O_{16}H_{27})$ and the order changes only after both OH groups turn to the trans position.

Summing up, the conformation change has a large effect on the geometry, on the atomic net charges, on the characteristic frequencies of the OH substituted ring, and on the molecular energy. The observed changes in the different properties of the OH substituted ring are in good accordance with each other.

Infrared spectra of the four PS conformers were simulated applying the calculated scaled frequencies and the quantum chemically calculated intensities applying Lorentz band functions with 15 cm^{-1} fwhh. Although the region below 1800 cm^{-1} contains fewer characteristic bands than the 3500 to 3000 cm^{-1} region, the conformation effect is observable quite well on the band shifts and in the changes in overlapping and resolving of the bands.

5. Conclusions

The molecular structure, the vibrational frequencies, and the vibrational force field of four pinosylvin conformers have been calculated. All of these conformers differing in the positions of the OH groups contain noncoplanar rings, i.e., the conjugation does not extend to the full skeleton of the molecule. The angle between the two rings increases going from the cis-cis to the trans-trans conformer. The break of the conjugation is reflected in several calculated properties. The rotation of the OH groups have negligible effect on the geometric parameters, the diagonal

TABLE 9: Vibrational Frequencies and Potential Energy Distributions of trans-trans Pinosylvin

wavenumber/cm^{-1}			wavenumber/cm^{-1}		
meas.	calc.	PED/% (distributions ≥ 5%)	meas.	calc.	PED/% (distributions ≥ 5%)
3405	3402	νOH 99 O16−H27 stretching	995	988	νrg 35 βrg 56
3397	3401	νOH 99 O18−H28 stretching	987	985	νrg 40 βrg 47 τCHv 7
3103	3114	νCHr 99 C4−H17 stretching	979	979	τCHr 17 τCHv 66
3103	3091	νCHr 99 unsubstituted ring stretching	964	962	τCHr 73 τCHv 11
3082	3081	νCHr 99 unsubstituted ring stretching	914	938	τCHr 97
3082	3073	νCHr 99 unsubstituted ring stretching	909	900	τCC 9 τCHr 69 τCHv 12
3060	3064	νCHr 99 unsubstituted ring stretching	864	862	τCC 7 τCHr 27 τCHv 59
3060	3062	νCHr 97 C6−H19 stretching	851	848	νrg 34 νCC 14 βrg 19 βCC 17
3056	3056	νCHr 99 unsubstituted ring stretching	829	825	τCHr 96
3056	3050	νCHr 96 C2−H15 stretching	819	817	τCHr 72 τCO 10
3029	3042	νCHv 94 anti-phase stretching	771	776	τCHr 74 τCO 9
3029	3035	νCHv 97 in-phase stretching	751	771	τCC 11 τCHr 67 τCO 9
1674	1671	νrg 8 νCC 66 βCHv 19	746	744	τrg 17 τCC 12 τCHr 59 τCHv 7
1637	1628	νrg 62 βrg 9 βCHr 12	693	693	νrg 20 νCC 8 νCO 8 βrg 35 βCC 19
1618	1622	νrg 68 βrg 9 βCHr 12	688	687	τrg 70 τCHr 28
1601	1615	νrg 66 βrg 9 βCHr 14	675	666	τrg 84
1588	1592	νrg 68 βrg 8 βCHr 17	619	618	νrg 10 βrg 84
1516	1522	νrg 37 βCHr 27 βCO 8 βOH 14	597	597	τrg 14 τCO 74
1494	1492	νrg 36 βCHr 56	585	593	τrg 25 τCC 41 τCO 29
1472	1462	νrg 46 νCO 10 βCHr 20	578	569	νrg 18 νCC 7 νCO 13 βrg 45
1448	1448	νrg 40 βCHr 47	551	551	βrg 16 βCC 32 βCO 38
1363	1374	νrg 63 βCHv 9 βOH 11	522	520	νrg 9 βrg 77
1358	1366	νrg 32 νCC 14 νCO 31 βrg 12	499	506	νrg 7 νCO 7 βrg 75
1341	1340	νrg 77 βCHr 12	487	486	τrg 50 τCC 39
1328	1322	νCC 15 βCC 9 βCHr 28 βCHv 45	427	419	νrg 10 βCC 55 βCO 22
1314	1310	βCC 11 βCHr 53 βCHv 22	401	401	τrg 98
1306	1297	νrg 8 βCC 7 βCHr 50 βOH 21	376	368	τOH 94
1256	1260	νrg 18 νCC 19 βCHr 16 βCHv 26 βOH 8	355	360	τOH 95
1210	1211	νrg 21 νCC 17 βCHr 16 βCHv 30	334	336	νrg 12 βrg 10 βCO 70
1201	1199	νrg 13 νCO 24 βCHr 33 βOH 25	288	289	τrg 57 τCC 24
1187	1189	νrg 18 βOH 65	247	242	νrg 9 νCC 13 βCC 21 βCO 7 τrg 33
1177	1170	νrg 20 βCHr 75	238	238	νCC 8 βCC 8 τrg 55
1170	1158	νrg 15 νCC 18 βCHr 51	222	223	τrg 76 τCO 8
1157	1146	νrg 14 βCHr 84	205	202	τrg 40 τCC 24 τCHv 8 τCO 23
1150	1131	νrg 8 νCO 25 βCHr 47 βOH 17	178	176	νrg 7 νCC 13 βrg 8 βCC 60
1074	1079	νrg 50 βCHr 42	84	87	βCC 24 τrg 9 τCHv 61
1028	1028	νrg 72 βCHr 23	57	56	βCC 70 τCHv 17
1007	1009	νrg 43 νCC 8 νCO 15 βCHr 15	51	51	τrg 9 τCC 86
999	993	νrg 37 νCC 9 νCO 14 βrg 20 βCHr 9	14	15	τCHv 97

[a] Mean deviation 5.07 cm^{-1}. Mean relative deviation 0.58%. [b] ν: stretching, β: in-plane deformation, γ: out-of-plane deformation, τ: torsion, CC: at least one carbon atom does not belong to ring; v: vinylidene group; r, rg: ring. [c] Wavenumbers below 200 cm^{-1} are chosen as equal to the for CT calculated ones.

TABLE 10: Changes in the Characteristic Vibrational Frequencies of the Substituted Ring of PS[a]

	vibrational frequencies/cm^{-1}			
normal mode	CC	CT	TC	TT
νC_2H_{15}	3092	3092	3050	3050
νC_4H_{17}	3035	3076	3075	3114
νC_6H_{19}	3103	3056	3103	3062
$\nu O_{16}H_{27}$	3402	3400	3401	3402
$\nu O_{18}H_{28}$	3405	3401	3403	3401

[a] PS: pinosylvin, CC: cis-cis, CT: cis-trans, TC: trans-cis, TT: trans-trans.

stretching force constants, and the charge distribution of the unsubstituted ring.

The change of the conformation from cis to trans in the OH group positions results in changes in some properties of the substituted ring. This transition causes electron repulsion in the direction of the vinylidene group and has a remarkable effect on the diagonal stretching force constants of the substituted ring.

As apparent from the results of the normal coordinate analysis, the CH stretching modes of the two rings are not coupled, although these modes of the unsubsituted ring are coupled with each other. The OH groups of the substituted ring isolate the CH groups. Therefore, based on the PED, it can be concluded that no coupling exists between them. While the calculated CH stretching frequencies of the substituted ring show a conformation effect, the OH stretching frequencies remain practically constant.

In contrary to our expectation, the CT conformer has the lowest molecular energy. The highest energy of the CC conformer is apparent because of the H−H repulsion between the hydrogen of the CH group and the two OH hydrogens.

Acknowledgment. The authors thank professors G. N. Andreev, B. N. Jordanov, and G. Keresztury for their help in the assignment of the vibrational spectra of trans-stilbene.

References and Notes

(1) Patent submitted to German Patent Buro, No. 19836774.0.

(2) Kuroda, H.; Kuroda, K., *Abstract Book of 7th International Congress on Plant Pathology*, Edinborough Univesity, 1998; abstract No. 1.14.1.

(3) Holmgren, A.; Bergström, B.; Gref, R.; Ericsson, A. *J. Wood Chem. Technol*. **1999**, *9*, 139.

(4) Schröder, J. *Nature Sruct. Biol*. **1999**, *6*, 714.

(5) Baranović, G.; Meić, Z.; Günsten, H.; Mink, J.; Keresztury, G. *J. Phys. Chem.* **1990**, *94*, 2833.

(6) Spoliti, M.; Bencivenni, L.; Quirante, J. J.; Ramondo, F. *THEOCHEM* **1997**, *390*, 139.

(7) Andreev, G. N.; Korte, E. H.; Jordanov, B. N.; Schrader, B. *J. Mol. Struct.* **1997**, *408/409*, 305.

(8) Baranović, G.; Meić, Z.; Maulitz, A. H. *Spectrochim Acta Part A* **1998**, *54*, 1017.

(9) Negri, F.; Orlandi, G. *J. Raman Spectrosc.* **1998**, *29*, 501.

(10) Mohammed-Ziegler, I. *Adsorption of Pinosylvin onto the Structure of Wood − Mechanism and Adsorption Parameters*, Licentiate Thesis, Luleå University of Technology, Luleå, Sweden, 2000.

(11) Frisch, M. J.; Trucks, G. W.; Schlegel, H. B.; Scuseria, G. E.; Robb, M. A.; Cheeseman, J. R.; Zakrzewski, V. G.; Montgomery, J. A. Jr.; Stratmann, R. E.; Burant, J. C.; Dapprich, S.; Millam, J. M.; Daniels, A. D.; Kudin, K. N.; Strain, M. C.; Farkas, O.; Tomasi, J.; Barone, V.; Cossi, M.; R. Cammi;, Mennucci, B.; Pomelli, C.; Adamo, C.; Clifford, S.; Ochterski, J.; Petersson, G. A.; Ayala, P. Y.; Cui, Q.; Morokuma, K.; Malick, D. K.; Rabuck, A. D.; Raghavachari, K.; Foresman, J. B.; Cioslowski, J.;. Ortiz, J. V.; Stefanov B. B.,; Liu, G.; Liashenko, A.; Piskorz, P.; Komaromi, I.; Gomperts, R.; Martin, R. L.; Fox, D. J.; Keith, T.; Al-Laham, M. A.; Peng, C. Y.; Nanayakkara, A.; Gonzalez, C.; Challacombe, M.; Gill, P. M. W.; Johnson, B.; Chen, W.; Wong, M. W.; Andres, J. L.; Gonzalez, C.; Head-Gordon, M.; Replogle, E. S.; and Pople, J. A.; *Gaussian 98*, Rev A.3; Gaussian, Inc.: Pittsburgh, PA, 1998.

(12) Hoekstra, A.; Meertens, P.; Vos, A. *Acta Crystallogr.* **1975**, *B31*, 2813.